Monitoring of Lubricant Film Failure in a Ball Bearing Using Ultrasound

Jie Zhang

Bruce W. Drinkwater[1]
e-mail: b.drinkwater@bristol.ac.uk

Department of Mechanical Engineering,
University of Bristol,
Bristol BS8 1TR,
United Kingdom

Rob S. Dwyer-Joyce
Department of Mechanical Engineering,
University of Sheffield,
Mappin Street,
Sheffield S1 3JD,
United Kingdom

A lubricant-film monitoring system for a conventional deep groove ball bearing (type 6016, shaft diameter 80 mm, ball diameter 12.7 mm) is described. A high-frequency (50 MHz) ultrasonic transducer is mounted on the static outer raceway of the bearing. The transducer is focused on the ball-raceway interface and used to measure the reflection coefficient of the lubricant in the "contact" ellipse between bearing components. The reflection coefficient characterizes the lubricant film and can be used to calculate its thickness. An accurate triggering system enables multiple reflection measurements to be made as each lubricated contact moves past the measurement location. Experiments are described in which bearings were deliberately caused to fail by the addition of acetone, water, and sand to the lubricant. The ultrasonic reflection coefficient was monitored as a function of time as the failure occurred. Also monitored were the more standard parameters, temperature and vibration. The results indicate that the ultrasonic measurements are able to detect the failures before seizure. It is also observed that, when used in parallel, these monitoring techniques offer the potential to diagnose the failure mechanism and hence improve predictions of remaining life. [DOI: 10.1115/1.2197848]

Keywords: bearing failure, lubricant film, condition monitoring, ultrasound

1 Introduction

A fluid lubricant, such as a synthetic or mineral oil, has several functions in a rolling element bearing. It provides elastohydrodynamic lubrication between the races and the rolling elements and hydrodynamic lubrication between the cage or separator and its locating surface. It serves as a coolant if either circulated through the bearing to an external heat exchanger or simply brought into contact with the bearing housing and the machine casing. A circulating lubricant also serves to flush out wear debris and carry it to a filter where it can be removed from the system. It also provides corrosion protection [1]. If the lubricant film at the rolling element "contact" collapses for any length of time, then heating and wear of the contacting components occurs rapidly and eventually the bearing will fail [2]. Bearing condition monitoring is therefore of major interest to a range of industries, particularly those continuously operating expensive and safety-critical plants such as those in the marine, power generation, and process sectors.

The traditional bearing monitoring techniques of temperature, vibration, and acoustic emission sensing, as well as wear debris analysis, measure the resultant effect of a failed or partially failed bearing [2,3]. Damage to the bearing surfaces and/or a loss or degradation of the lubricant cause increases in the temperature of the bearing and its average vibration level. Recent years have seen a number of workers utilize a range of novel nondestructive techniques to aid the early measurement of bearing failure and diagnose its cause. For example, Miettinen et al. [4,5] used acoustic emissions to monitor rolling bearings, the concept being that any ball-raceway contact and production of wear debris produce high-frequency sound.

Researchers have used a range of techniques to monitor lubricant film thickness such as optical [6,7], capacitance [8,9], and eddy currents [10]. These approaches have the attraction that they provide additional information to the traditional techniques (and acoustic emission) and offer the potential to give early warning of failure and/or other diagnostic information. However, these techniques have all proved difficult to implement in practice, particularly in rolling element bearings where submicron oil films are expected. Recently Anderson et al. [11] used the transmission (and reflection) of transverse ultrasonic waves to monitor the collapse of oil layers in thin fluid shaft seals. The principle is that the presence of the lubricant causes significant reflection of the ultrasound and, so, on collapse an increase in the transmitted ultrasonic energy is seen. This approach has been shown to be entirely noninvasive and applicable to many industrial bearings.

Dwyer-Joyce et al. [12] and Zhang et al. [13,14] demonstrated that ultrasonic reflection coefficient measurements can be used to monitor the lubricant-layer thickness in rolling element bearings. These bearings were in the elastohydrodynamic (EHD) regime and the lubricant film was in the range 0.3–1.0 μm. The bearings were run under normal operating conditions and results were shown to agree well with models of the bearing performance.

This paper demonstrates the on-line monitoring of lubricant film failure in rolling element bearings using ultrasound. This is a critical step forward from previous studies in which the bearing was operating normally. As the bearing failed, the temperature of the bearing and the vibration of the bearing housing are also measured simultaneously. The results are used to explain the failure process of the ball bearing. This has significant implications for the diagnosis of bearing failure mechanisms and the prediction of remaining life in a wide range of industrial plant monitoring applications.

2 Background Theory

2.1 Ultrasonic Reflection From a Lubricant Layer. When high-frequency ultrasonic waves are incident on a ball bearing system their interactions with the lubricant film can be described by the following three-layered system; "outer raceway"-"lubricant-layer"-"ball". In terms of materials this system is typically steel-oil-steel. If the thickness of the lubricant layer is small in comparison with the ultrasonic wavelength, the media on either

---

Table 1 Acoustic properties of Shell T68 lubricating oil, steel, and air

	Density ρ (kg/m³)	Longitudinal wave velocity c (m/s)	Bulk modulus B (GPa)
Oil at 0.1 MPa	876	1460	1.84
Oil at 0.8 GPa	1002	3550	12.6
Oil at 1.5 GPa	1044	4500	21.2
Steel (EN24)	7900	5900	172
Air (20°C)	1.3	330	1.42e−4

Fig. 1 Geometry of the lubricated "contact" region of the ball bearing and the region of focus of the 50 MHz ultrasonic transducer

side of the layer have identical acoustic properties, and the ultrasound is normally incident, then the well-known quasi-static spring model can be used [14]. In this way, the modulus of the measured reflection coefficient, $|R|$, is related to the acoustic properties of the three-layer system by [15]:

$$|R| = \sqrt{\frac{\left(\frac{\pi h f z}{B}\right)^2}{1+\left(\frac{\pi h f z}{B}\right)^2}} \qquad (1)$$

where h is the lubricant film thickness, z is the acoustic impedance of the surrounding medium (i.e., steel), f is the ultrasonic frequency at which the measurement is made, and B is the bulk modulus of the lubricant. Note also that $B = \rho c^2$, where ρ and c are the density and speed of sound in the lubricant layer, respectively. From Eq. (1), it can be seen that for a given bearing, at a given frequency, the reflection coefficient changes only with the bulk modulus and thickness of the lubricant layer. The use of ultrasonic reflection coefficient measurements for bearing monitoring therefore inherently assumes that a number of bearing failure mechanisms are characterized by a change in either the bulk modulus or the lubricant-layer thickness. In this way the change of the reflection coefficient can be used to help diagnose the failure mechanics and to provide warning prior to failure.

The reflection coefficient is usually obtained with respect to a reference measurement from a known interface by:

$$R(f) = \frac{A_m(f)}{A_{ref}(f)} R_{ref} \qquad (2)$$

where $A_m(f)$ is the amplitude of the signal reflected from the lubricant film, $A_{ref}(f)$ is the amplitude of the reference signal, and R_{ref} is the reflection coefficient of the reference interface. Typically $A_m(t)$ would be measured by first isolating in time the signal reflected from the lubricant film from any other signals and converting this to the frequency domain via a fast Fourier transform (FFT) to obtain $A_m(f)$. As wideband ultrasonic transducers are used, so the reflection coefficient can be measured over a range of frequencies. However, to maximize the speed of the measurement, in this paper only the center frequency of the transducer (50 MHz) is considered. The reference measurement is taken in a similar way, using the signal reflected from a steel-air interface obtained prior to the addition of the lubricating oil at the start of the experiment. For this system the reference reflection coefficient, R_{ref},
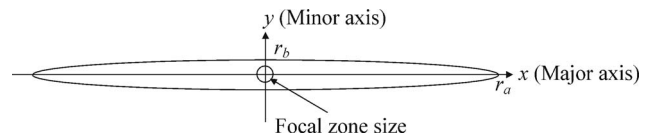
is that from the steel-air interface that, using the material properties shown in Table 1, was found to be 0.99998.

2.2 The Lubricated Contact Region in a Ball Bearing. The geometry of the lubricated contact that forms when a ball is pressed onto a closely conforming raceway groove can be calculated from the applied load, P, the bearing geometry and mechanical properties, and the lubricant properties [2]. Figure 1 shows the geometry of the lubricated contact region of a ball bearing. For the bearing used in this paper (type 6016 deep groove), the lubricated contact region is elliptical in shape with the major (r_a) and minor (r_b) semi-contact radii given by:

$$r_a = \left(\frac{6k^2 \varepsilon P R'}{\pi E'}\right)^{1/3}, \quad r_b = \left(\frac{6\varepsilon P R'}{\pi k E'}\right)^{1/3} \qquad (3)$$

where k and ε are measures of the shape of the contact ellipse obtained from look-up tables [2] and given in Table 2. E' is the reduced elastic modulus and R' is the reduced radius of curvature given by:

$$\frac{1}{E'} = \frac{1}{2}\left(\frac{1-\nu_a^2}{E_a} + \frac{1-\nu_b^2}{E_b}\right), \quad \frac{1}{R'} = \frac{1}{R_{ax}} + \frac{1}{R_{bx}} + \frac{1}{R_{ay}} + \frac{1}{R_{by}} \qquad (4)$$

where E is Young's modulus, ν is Poisson's ratio, R is the radius of the two rolling elements (subscripts a and b refer to the ball and raceway respectively), and x and y are the coordinate axes shown on Fig. 1.

The geometry of the ball and raceway is such that the major semi-contact width r_a is around ten times the minor semi-contact width r_b. As shown in Fig. 1, the elliptical contact of a given ball moves around the raceway in the y-direction and so the ultrasonic measurements are made across the minor axis of the contact ellipse. The pressure distribution over the elliptical region is given by [16]:

$$p = p_0 \sqrt{1 - \left(\frac{x}{r_a}\right)^2 - \left(\frac{y}{r_b}\right)^2} \qquad (5)$$

where p_0 is the maximum contact pressure which occurs at the center of the contact ellipse. The load on the ball is not the same as that on the whole bearing because several balls are in contact with the raceways at any instant. The ultrasonic transducer is positioned directly opposite the point of load application and so the load on the ball is given by the well-known Stribeck equation (see for example [3]):

Table 2 Parameters required to calculate the theoretical lubricant-film thickness via the Dowson and Higginson equation [2,17]

Reduced modulus E' (GPa)	Reduced radius R' (m)	Pressure viscosity coefficient α (GPa−1)	Ellipticity parameter k	Simplified elliptical integrals ε	Effective viscosity η_0 (N/m²s)
228	5.85e-3	20	11.5	3.8	0.2

$$P = \frac{5W}{n} \tag{6}$$

where W is the radial load on the whole bearing and n is the number of the balls in the bearing. The mean and peak contact pressures are then given by:

$$p_m = \frac{P}{\pi r_a r_b} \quad \text{and} \quad p_0 = \frac{3P}{2\pi r_a r_b} \tag{7}$$

For a ball bearing, operating in the elastohydrodynamic lubrication regime, the lubricant film thickness can be estimated from the numerically derived regression equations of Hamrock and Dowson [17]. They showed that the central film thickness, h_c, can be expressed as:

$$\frac{h_c}{R'} = 2.69 \left(\frac{U\eta_0}{E'R'} \right)^{0.67} (\alpha E')^{0.53} \left(\frac{P}{E'R'^2} \right)^{-0.067} (1 - 0.61 e^{-0.73k}) \tag{8}$$

where U is the mean surface speed, η_0 is the lubricant viscosity at the contact entry, α is the pressure-viscosity coefficient, k is an ellipticity parameter, and P is the load on the measured ball obtained from Eq. (6).

Pressures in the ball bearing lubricated contacts are high, and this has the effect of increasing both the density and the bulk modulus of the lubricant. The latter parameter is required for the determination of the film thickness ultrasonically from the reflection coefficient (Eq. (1)). Jacobson and Vinet [18] developed a model for this bulk modulus variation with pressure. They give an equation of state to describe the behavior of the lubricant under pressure, p:

$$p = \frac{3B_0}{s^2} (1 - s) e^{t(1-s)} \tag{9}$$

and the bulk modulus under pressure is given by:

$$B = \frac{B_0}{s^2} [2 + (t-1)s - st^2] e^{t(1-s)} \tag{10}$$

where B_0 is the bulk modulus at zero pressure, t is a lubricant specific parameter, and s is a function of the relative compression:

$$s = \sqrt[3]{\frac{\rho_o}{\rho_p}} \tag{11}$$

where ρ_0 is the density at zero pressure, and ρ_p at pressure p. The parameter t is determined empirically from tests on lubricants in high pressure cells (pressures up to 2.2 GPa were reported in [18]).

Substituting Eq. (9) into Eq. (10) allows the relationship between pressure and bulk modulus to be expressed as,

$$B = \frac{[2 + (t-1)s - st^2]}{3(1-s)} p \tag{12}$$

From Eq. (12), it can be seen that there is linear relationship between bulk modulus and pressure. Because of the experimental complexities, bulk modulus as a function of pressure data is scarce; in this paper data available for an oil of a similar generic type [18] to that used in the experiments are used. Table 1 shows the bulk modulus determined at three contact pressures using this analysis.

3 Ball Bearing Experimental Apparatus

An experimental apparatus capable of accurately measuring the ultrasonic reflection coefficient from a lubricant film in a 6016 bearing system is shown in Fig. 2. The bearing test rig consisted of a rotating shaft of 80 mm diameter supported on four 6016 ball bearings and ultrasonic transmit-receive instrumentation. As shown in Fig. 2, bearings 1 and 4 were fitted to the ends of the shaft and fixed into rigid housings. Radial loads were applied to
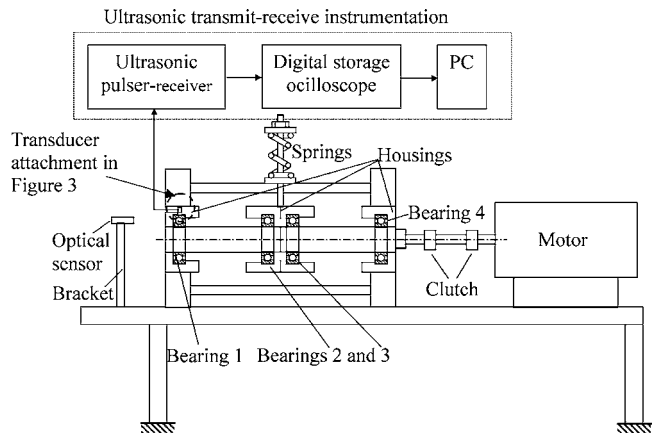
Fig. 2 Schematic diagram of the experimental apparatus made up of four 6016 ball bearings

the shaft through bearings 2 and 3. The load was applied vertically upwards by an arrangement of compressed springs. In this way the balls at the top of bearings 1 and 4 were the most heavily loaded. The rotary shaft speed was controllable in the range 100–2900 rpm by a 7.5 kW electric motor. The bearing was lubricated with Shell T68 mineral oil (details shown in Table 1) using a total loss gravity feed system. Bearing 1 was instrumented with the ultrasonic measurement system. An optical sensor was used, both to allow accurate triggering of the ultrasonic instrumentation and to measure shaft speed.

Figure 3 shows the ultrasonic measurement system fitted to bearing 1 in more detail. A focused, longitudinal wave piezoelectric ultrasonic transducer (Valpey Fisher 50 MHz) was mounted in a small hole (17 mm diameter) drilled though the bearing housing such that it was normal to the top surface of the outer raceway. This transducer acted as both an emitter and receiver (pulse-echo mode) and had a center frequency of 50 MHz, an active element diameter of 5 mm, and a focal length in water of 23 mm. This equates to a theoretical focal spot size (defined at −6 dB down from the maximum) in the plane of the lubricant film of 146 μm at the center frequency. The transducer was selected to ensure that the focal spot size was less than the minor lubricated contact diameter. Note that the upper operating frequency is not infinitely variable but is limited by material attenuation and sensitivity to small angular misalignments, which both increase with frequency.
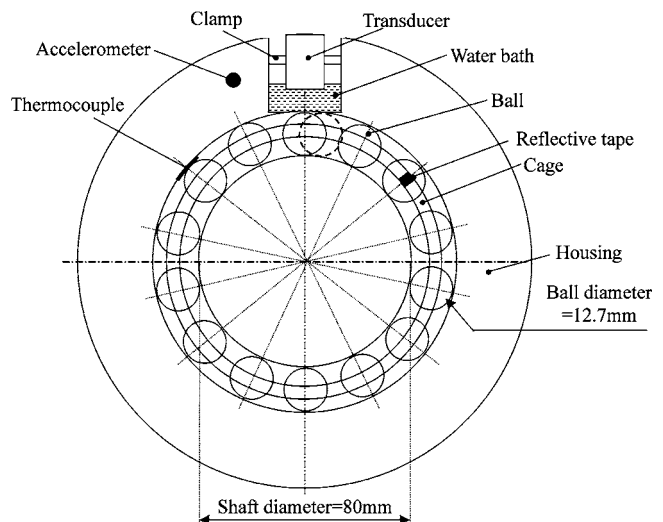
**Fig. 3 Transducer attachment and bearing geometry**

Experience from the nondestructive testing community [19] indicates that 50 MHz is close to the upper operating limit for use with steel components. The ultrasonic transducer was connected to a pulser-receiver (type Panametrics 5072PR). This outputs a Dirac delta function-like voltage spike containing energy in the range 5–200 MHz to excite the transducer and contains a receive amplifier to condition the reflected signals. The waveform was then digitized at 250 Msamples/s and passed to a PC for storage and analysis.

Also shown in Fig. 3 is the reflective tape attached to the bearing cage. When this tape passed an optical sensor it generated a 5 V positive pulse that then triggered a signal generator (type Agilent 33220A). After the addition of an adjustable delay the signal generator then triggered the pulser-receiver at its maximum pulse repetition frequency, which was 20 kHz. By triggering in this way, a number of ultrasonic pulses were used to interrogate the lubricated contact region as a ball passed under the transducer. The delay between the optical trigger and the ultrasonic pulsing was adjusted by knowledge of the shaft speed and the distance between the trigger point (the reflective tape) and the focal spot of the transducer. In this way a reflection coefficient profile was measured for each lubricated contact region, the number of points in the profile being governed by the rotational speed of the bearing. An accelerometer and thermocouple were also attached to the bearing to monitor the vibration and temperature, respectively, and their locations are shown in Fig. 3. The accelerometer was positioned to measure horizontal vibration of the bearing and housing and the thermocouple was positioned to measure the temperature of the outer raceway of the bearing close to the position of the ultrasonic transducer.

4 Results and Discussion

4.1 Reflection Coefficient Profile and Thickness Profile Measurement. The failure of rolling element bearings is frequently associated with lubrication failure, ingress of water, or contamination by hard particles. These processes result in an inadequate separation of the rolling elements and raceways leading to wear, contact fatigue, and surface damage. In order to replicate these failure mechanisms in the laboratory, three contaminant materials (acetone, water and sand) were added to the oil in order to initiate rapid failure of the ball bearing. These three contaminants were chosen as it was anticipated that they would result in different failure scenarios. Acetone dissolves in the lubricant and reduces its viscosity. It also acts to flush out the oil from the bearing. Water does not dissolve in the oil but causes rapid corrosion of the bearing parts as well as reducing the apparent viscosity of the oil. It also acts to flush out the oil from the bearing. Sand directly damages the bearing surfaces through abrasion. Particle diameters of 50 μm were used to ensure that they were greater than the size of the lubricant film to increase their wear properties.

Figure 4(a) shows an experimentally measured reflection coefficient profile for a shaft speed of 506 rpm and a bearing radial load of 15 kN before any contaminant materials were added to the lubricant. Reflected signals were recorded at a rate of 20 kHz as the ball passed the transducer location. It can be seen that the reflection coefficient falls to a minimum at the center of the lubricated contact region and then rises again. This minimum reflection coefficient corresponds to an oil film thickness of 0.75 μm. Also shown in Fig. 4(a) is the theoretical reflection coefficient distribution (using Eq. (8) to obtain thickness, then Eq. (1) to calculate the reflection coefficient). Note that for the theoretical line, the central film thickness has been assumed to occur across the whole of the contact (i.e., the minimum film thickness at the exit constriction of the contact is not modelled). Figure 4(b) shows an experimentally measured thickness profile and theoretical thickness profile corresponding to the reflection coefficient profile shown in Fig. 4(a). Comparing the two curves in Fig. 4(a) and the two curves in Fig. 4(b), it can be seen that there is a good quantitative agreement at
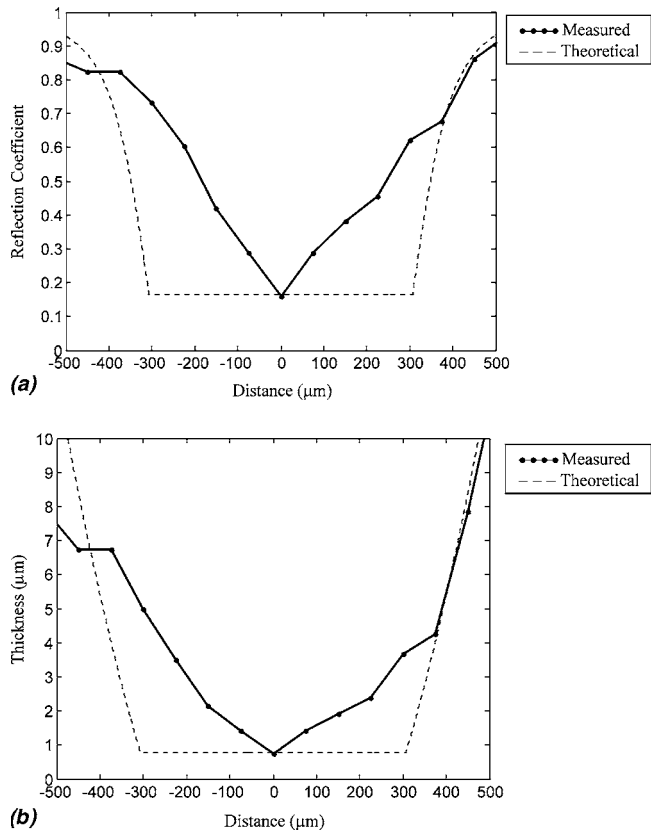
Fig. 4 Shaft speed of 506 rpm and a radial load of 15 kN. (a) Measured reflection compared with a theoretical prediction based on a predicted oil film thickness. (b) Measured lubricant thickness compared with a theoretical thickness.
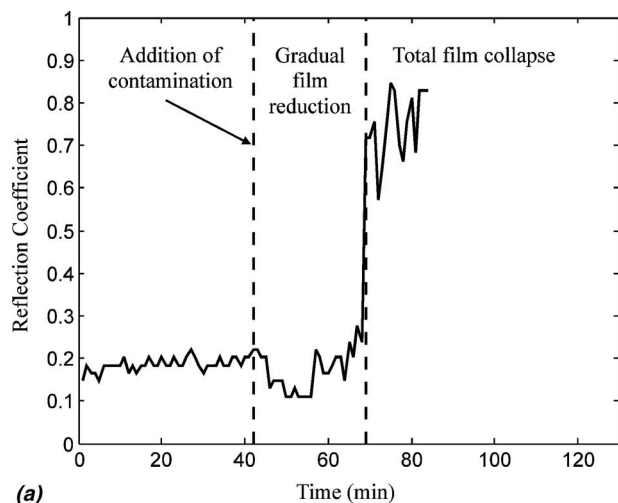
the center of the lubricated contact and poor agreement elsewhere. This is due to two distinct effects. Firstly, there will be errors in the theoretical line due to the assumption of constant lubricant thickness. Secondly, there are errors in the experimental line due to the averaging effect of the finite focal spot size of the ultrasonic beam (see [14] for fuller details). Note that both errors are minimized in the central region.

With the current experimental system it takes approximately 1 min to collect and process the data from each ball. As each of the 14 balls can be measured by adjusting the delay between the optical trigger and the ultrasonic pulsing, so it takes 14 min to cycle though all balls within the bearing.
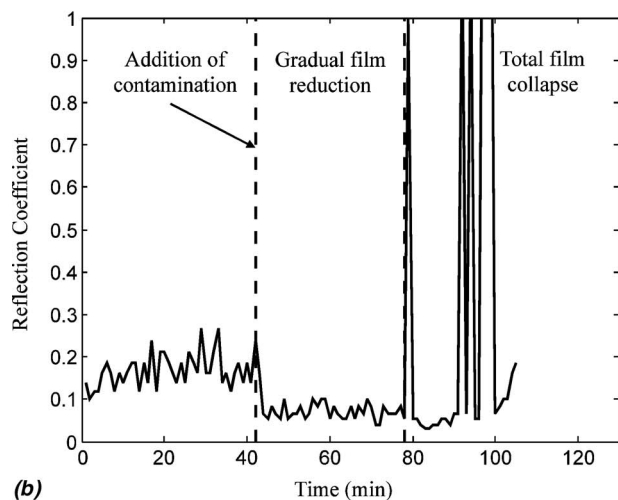
4.2 Monitoring the Failure Process. In order to compare the effect of different contaminants on the lubricant layer, an identical procedure was used for each test. In this procedure, contaminant materials were added to the lubricant feed after three monitoring cycles (i.e., after 42 min of normal operation). The contaminated oil was added at a rate of 5–10 ml/min. The acetone and water were used as the contaminated oil and the proportion of sand in the lubricant oil was 0.1–0.2 g/ml. In each case, the experiment finished when the ball bearing seized. Figures 5(a)–5(c) show the center reflection coefficient as a function of time for the three different failure cases. From Figs. 5(a)–5(c), it can be seen that in the first 42 min, there is only small variation of the reflection coefficient. This variation represents the measurement "noise" and corresponds to a 4% variation in the amplitude of the center reflection.

When acetone was added to the lubricant, it can be seen from Fig. 5(a) that the reflection coefficient first decreases (from an average of 0.18 to 0.14 shown as gradual film reduction regime) and then steeply increases after 69 min (shown as total film col-
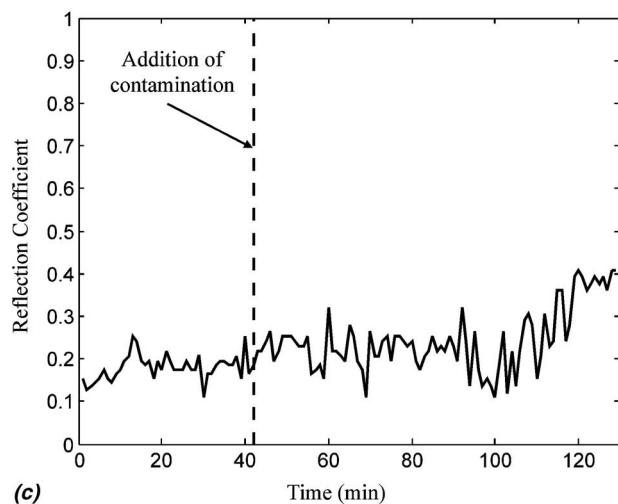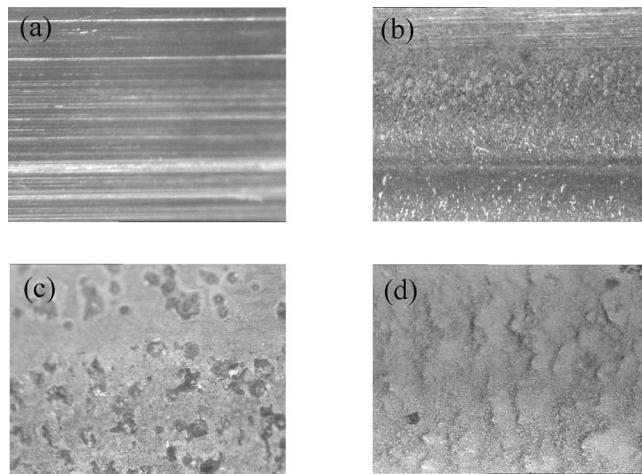
(a)

(b)

Fig. 5 Reflection coefficient versus time for failure by the addition of (*a*) acetone, (*b*) water, and (*c*) sand

(c)

(a)

(b)

(c)

(d)

Fig. 6 Photograph for a small contacting area at outer-raceway surface for different ball bearings (2.5×1.9 mm² of the surface is shown). (*a*) Undamaged surface, (*b*) after contamination by acetone, (*c*) after contamination by water, and (*d*) after contamination by sand.

Contact of the bearing surfaces would then result in a high wear rate and a roughening of the ball and raceway surfaces. Roughening of the bearing surfaces can be seen by comparing photographs of the surface of the outer raceway before (Fig. 6(*a*)) and after (Fig. 6(*b*)) contamination by acetone. This increased roughness and starved lubrication caused the ultrasonic wave to be mostly reflected from the interface, hence the observed dramatic increase in reflection coefficient [20].

When water was added to the lubricant, it can be seen from Fig. 5(*b*) that, as in the acetone case, the reflection coefficient initially decreases, followed by a series of sharp reflection coefficient peaks, starting after 42 min. The initial reduction in reflection coefficient is slightly more marked than for acetone (average reflection coefficient falling from 0.17 to 0.07 shown as gradual film reduction regime). It is likely that the water (since it is not piezo-viscous) will not enter the contact. However, some will dissolve in the oil, reducing its viscosity, and the water may also act to displace lubricating oil from the contact inlet. Both these effects would cause a reduction in the film thickness and hence a reduction in the reflection coefficient. The reflection coefficient remains at this reduced value for 78 min (until the point marked as total film collapse). With time the surfaces of the raceway and ball oxidize, leading to increased wear and damage (increased surface roughness). This oxidation can be seen in Fig. 6(*c*). The presence of oxidation products and the increased surface roughness acting together then cause the observed dramatic increases in the reflection coefficient.

Figure 5(*c*) shows the effect of the addition of sand particles to the lubricant. This causes a gradual increase in the reflection coefficient over the 125 min duration of the test. The sand particles roughen the contacting surfaces; the roughness changes from Ra =0.02 μm to Ra=0.14 μm. Figure 6(*d*) shows a photograph of the bearing surface after the addition of sand to the bearing. It appears that this roughening of the surface has led to a slight increase in the measured film thickness. The reflection coefficient is sensitive to the separation of the mean lines of the two rough surfaces. With the increased roughness and the possibility of micro-elastohydrodynamic lubrication at the asperity contacts, the measured film thickness and hence reflection coefficient increases marginally. The sand abrasion also caused an increase in the radii of the contact elements and hence a decrease in the contact pressure (Eq. (5)). The film thickness therefore increases slightly, and the reflection coefficient also increases.

It is now instructive to compare the ultrasonic results shown in

lapse regime). The bearing seized after 84 min, which was the shortest of the three contaminant cases. The failure scenario is as follows. First, the acetone dissolves the lubricant, which lowers its viscosity and hence reduces the lubricant film thickness resulting in an immediate decrease in the reflection coefficient. Second, over the next 12 min it is thought that the acetone and lubricant evaporate, causing a lack of lubrication of the bearing to occur.
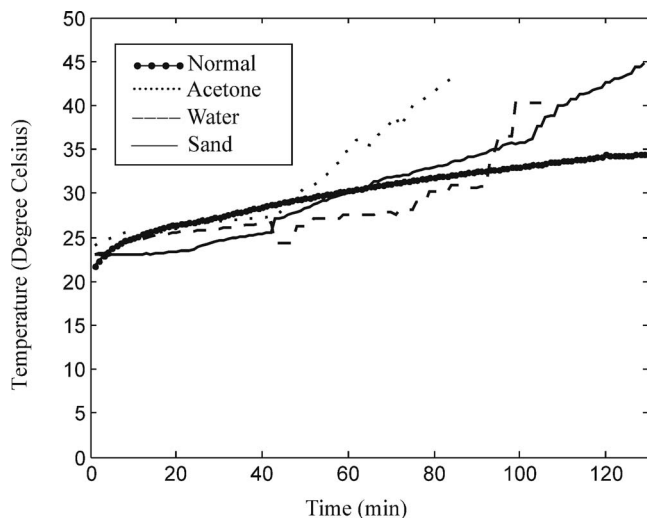
Fig. 7 Temperature versus time for a ball bearing under normal operation (labelled "normal") and various failure cases

Figs. 5(a)–5(c) with more conventional condition monitoring approaches of temperature and vibration sensing. Figure 7 shows the variation in temperature as a function of time for the same three failure cases. It can be seen that the temperature increases gradually for all contaminant cases and for normal operation. The most marked change is for the addition of acetone and that can be seen to result in a significant change in the gradient of temperature increase. This is in agreement with the hypothesis that the evaporation of the acetone caused the bearing to be starved of lubricant and hence significant heating though solid-solid contact resulted. The acetone also resulted in the most rapid seizure of the bearing. The addition of water causes a small initial effect (a reduction in temperature) followed by a similar gradient to that seen before its addition. However, after 92 min the temperature starts to increase more rapidly. This coincides with the observed dramatic increase in reflection coefficient seen in Fig. 5(b). From Fig. 7 it can be seen that the addition of sand caused a small increase in the gradient of temperature increase. It can also be seen that the gradient further increases after 90 min, presumably due to an increased rate of wear prior to failure.
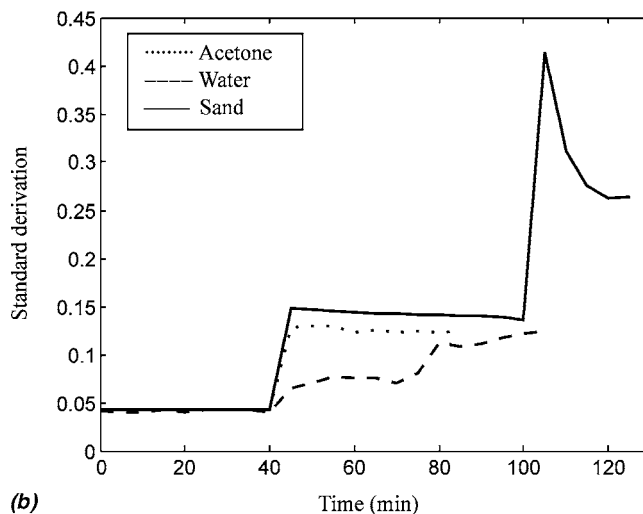
Figure 8 shows typical vibration signals before and after the addition of sand to the lubricant from which a significant increase in vibration amplitude is clear. Figure 9 shows the vibration mea-
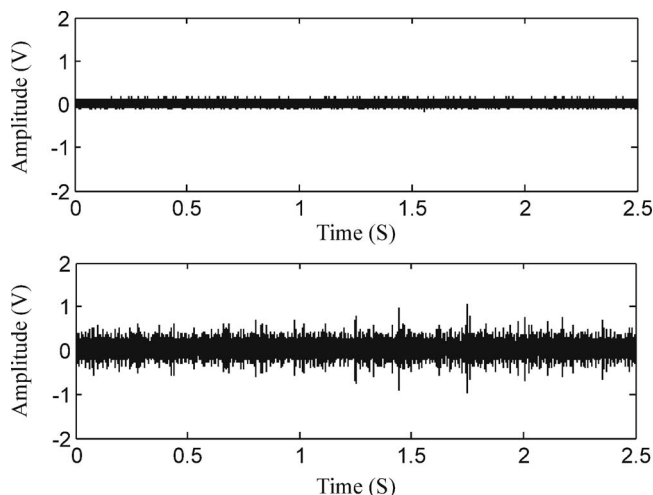
Fig. 8 Vibration signals before and after failure for sand case
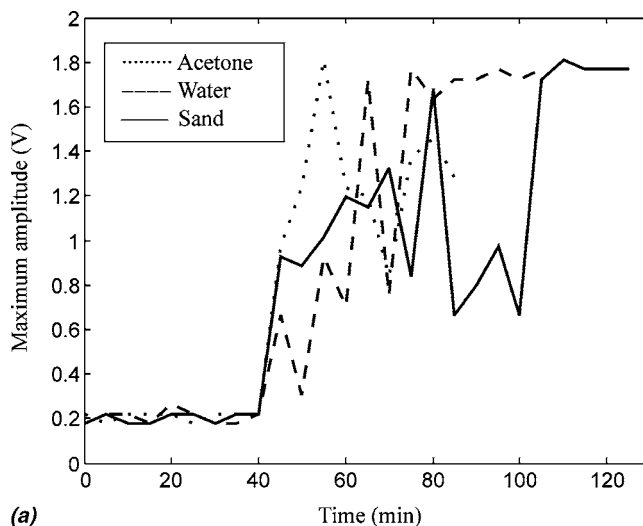
Fig. 9 Vibration signals versus time for various failure cases: (a) maximum amplitude and (b) standard derivation

surements for the three tests. From Fig. 9(a) it can be seen that the maximum vibration level increases after the addition of all three contaminants. Although this may be useful in some circumstances, this measure is not very discriminating. Figure 9(b) shows the standard deviation of the vibration measurements. From this figure it can be seen that, as expected, the addition of sand causes the most clear increase in vibration. The addition of acetone also results in significant vibration, probably due to the high speed of the failure commented on earlier. The effect of the addition of water is the smallest of the three cases.

The results of Figs. 5(a)–5(c) are presented as reflection coefficients. It is possible to convert this to oil film thickness provided the bulk modulus of the oil in the contact is known. Values for the bulk modulus have been determined for the uncontaminated lubricant (i.e., up to 42 min in Figs. 5(a)–5(c)) and this corresponds to an oil film thickness of 0.75 μm. As soon as the contaminant is added the bulk modulus changes to an unknown value and, so, for the purposes of this study, the data have been left as reflection coefficients.

In both cases of liquid contamination the trend in reflection coefficient is the same. Immediately after the contaminant is introduced it falls. This corresponds to the sudden reduction in oil film thickness as the lower viscosity lubricant is entrained into the contact. After a short period of time the reflection coefficient rises to unity. For the acetone, this corresponds to the complete absence

of an oil film and so the ultrasonic pulses are now reflected from a steel-air interface. For the water the combination of increased surface roughness and the presence of oxidation products is thought to result in a similar increase in reflection coefficient.

Thus measurements of ultrasonic reflection coefficient can therefore be used in two ways. First, they can be used to monitor a gradual reduction in oil film. This might occur, for example, if the lubricant supply degrades with time. This provides an early warning that indicates corrective measures need to be taken at, say, the next maintenance shut down. Second, if the reflection coefficient rapidly increases to one, this indicates that there has been a sudden film collapse. Complete bearing failure by seizure is then likely and immediate action needs to be taken.

5 Conclusions

Usually lubricant film and machine element failure is observed by monitoring the effects of the failure through temperature, vibration, and acoustic emission measurement. In this paper the measurement of the ultrasonic reflection coefficient has been presented as an alternative. This technique has been shown to be sensitive to the thickness and bulk modulus of the lubricant film. In this way it is possible to characterize the lubricant film directly. Potentially this can be used to indicate the onset of failure before surface damage occurs. Ultrasonic reflection coefficient measurements have been used to monitor the lubricant film failure in a rotating element ball bearing (type 6016). The monitoring system allowed reflection coefficient distribution to be measured alongside vibration and temperature. For known operating conditions an accurate reflection coefficient was obtained from the center of the lubricated contact. Three contaminant materials (acetone, water, sand) were separately added to the lubricant to initiate failure of the bearing. These contaminants simulated common failure mechanisms that can occur in the field. The ultrasonic reflection coefficient, vibration, and temperature were recorded under these three failure scenarios. The ultrasonic reflection coefficient measurements were shown to provide useful diagnostic information on the failures, as well as an early warning signal. When used in conjunction with vibration and/or temperature an enhanced approach to on-line bearing degradation analysis and future life prediction is possible. The performance of the experimental system demonstrates that this technique has the potential for on-line condition monitoring of lubricant films in industrial applications.

Acknowledgment

References

[1] Hamrock, B. J., Schmid, S. R., and Jacobson, B. O., 2004, *Fundamentals of Fluid Film Lubrication*, 2nd ed., Marcel Dekker, New York, pp. 1–20.

[2] Stachowiak, G. W., and Batchelor, A. W., 2001, *Engineering Tribology*, Butterworth Heinemann, Woburn, MA, pp. 281–313.

[3] Harris, T. A., 2001, *Rolling Bearing Analysis*, 4th ed., Wiley, New York, Chap. 7, p. 238.

[4] Miettinen, J., Andersson, P., and Wikstrom, V., 2001, "Analysis of Grease Lubrication of a Ball Bearing Using Acoustic Emission Measurement," Proc. Inst. Mech. Eng., Part J: J. Eng. Tribol., **215**(6), pp. 535–544.

[5] Miettinen, J., and Siekkinen, V., 1995, "Acoustic Emission in Monitoring Sliding Contact Behaviour," Wear, **181–183**(2), pp. 897–900.

[6] Cameron, A., and Gohar, R., 1966, "Theoretical and Experimental Studies of the Oil Film in Lubricated Point Contact," Proc. R. Soc. London, Ser. A, **291**, pp. 520–536.

[7] Richardson, D. A., and Borman, G. L., 1991, "Using Fiber Optics and Laser Fluorescence for Measuring Thin Oil Films with Applications to Engines," Society of Automotive Engineers, SAE Paper No. 912388.

[8] Astridge, K. G., and Longfield, M. D., 1967, "Capacitance Measurement and Oil Film Thickness in a Large Radius Disc and Ring Machine," Proc. Inst. Mech. Eng., **182**, pp. 89–96.

[9] Dyson, A., 1967, "Investigation of the Discharge-Voltage Method of Measuring the Thickness of Oil Films Formed in a Disc Machine Under Conditions of Elastohydrodynamic Lubrication," Proc. Inst. Mech. Eng., **181**, pp. 633–645.

[10] Glavatskih, S. B., Uusitalo, O., and Spohn, D. J., 2001, "Simultaneous Monitoring of Oil Film Thickness and Temperature in Fluid Film Bearings," Tribol. Int., **34**(12), pp. 853–857.

[11] Anderson, W., Jarzynski, J., and Salant, R. F., 2000, "Condition Monitoring of Mechanical Seals: Detection of Film Collapse Using Reflected Ultrasonic Waves," Proc. Inst. Mech. Eng., Part C: J. Mech. Eng. Sci., **214**, pp. 1187–1194.

[12] Dwyer-Joyce, R. S., Drinkwater, B. W., and Donohoe, C. J., 2003, "The Measurement of Lubricant-Film Thickness Using Ultrasound," Proc. R. Soc. London, Ser. A, **459**, pp. 957–976.

[13] Zhang, J., Drinkwater, B. W., and Dwyer-Joyce, R. S., 2005, "Calibration of the Ultrasonic Lubricant Film Thickness Measurement Technique," Meas. Sci. Technol., **16**(9), pp. 1784–1791.

[14] Zhang, J., Drinkwater, B. W., and Dwyer-Joyce, R. S., 2006, "Acoustic Measurement of Lubricant-Film Thickness Distribution in Ball Bearings," J. Acoust. Soc. Am., **119**(2), pp. 863–871.

[15] Pialucha, T., and Cawley, P., 1994, "The Detection of Thin Embedded Layers Using Normal Incidence Ultrasound," Ultrasonics, **32**(6), pp. 431–440.

[16] Hill, D. A., Nowell, D., and Sackfield, A., 1992, *Mechanics of Elastics Contacts*, Butterworth Heinemann, Woburn, MA, Sec. 10.4, pp. 291–320.

[17] Hamrock, B., and Dowson, D., 1977, "Isothermal Elasto-Hydrodynamic Lubrication of Point Contact—Part III – Fully Flooded Results," ASME J. Lubr. Technol., **99**, pp. 264–276.

[18] Jacobson, B. O., and Vinet, P. A., 1987, "Model for the Influence of Pressure on the Bulk Modulus and the Influence of Temperature on the Solidification Pressure for Liquid Lubricants," ASME J. Tribol., **109**, pp. 709–714.

[19] Krautkramer, J., and Krautkramer, H., 1990, *Ultrasonic Testing of Materials*, Springer-Verlag, New York, pp. 304–306.

[20] Drinkwater, B. W., Dwyer-Joyce, R. S., and Cawley, P., 1996, "Study of the Interaction Between Ultrasound and a Partially Contacting Solid-Solid Interface," Proc. R. Soc. London, Ser. A, **452**, pp. 2613–2628.